Singlet Oxygen Generation by 8-Methoxypsoralen in Deuterium Oxide: Relaxation Rate Constants and Dependence of the Generation Efficacy on the Oxygen Partial Pressure

Roland Engl,[†] Robert Kilger,[†] Max Maier,[†] Kathrin Scherer,[‡] Christoph Abels,[‡] and Wolfgang Bäumler*[,‡]

Institute of Experimental and Applied Physics and Department of Dermatology, University of Regensburg, Regensburg, Germany

Received: October 5, 2001; In Final Form: March 8, 2002

The photoactivation of 8-methoxypsoralen (8-MOP) by ultraviolet light is widely used for the treatment of several skin diseases. The major mechanism is the intercalation of 8-MOP into nuclear DNA in the dark and subsequently the formation of monoadducts and potential cross links under UVA irradiation. In addition, the irradiation of 8-MOP leads to the generation of singlet oxygen by means of photodynamic action which has been shown to induce a critical oxidative damage of the DNA in vitro. To assess the role of singlet oxygen generated by photoactivated 8-MOP, its relaxation in solutions of deuterium oxide was studied in detail. Relaxation rates and rate constants of the involved 8-MOP triplet T_1 state and oxygen $^1\Delta_g$ state were determined by analyzing the rise and decay rates of the luminescence of singlet oxygen at 1.27 μm. The efficacy of singlet oxygen generation is described by the singlet oxygen quantum yield Φ_Δ, which depends on the efficacy of 8-MOP T_1 state deactivation by oxygen, $P_T([O_2])$. $P_T([O_2])$ has been determined for different oxygen concentrations and decreased from 2% under aerated conditions (e.g., in vitro conditions, 130 Torr) to 0.5% for the *in vivo* situation inside the skin (~20 Torr). The efficacy of singlet oxygen generation and maybe therefore the role of singlet oxygen in the oxidative damage depends critically on the respective oxygen partial pressure. This must be considered when transferring results and conclusions from experiments in vitro or in solution to the situation in vivo.

1. Introduction

Among the group of psoralen derivatives, the linear furocoumarin 8-methoxypsoralen (8-MOP) is used extensively for the clinical treatment of psoriasis and several other skin disorders including vitiligo, mycosis fungoides, and eczema.[1] This treatment, called PUVA therapy (psoralen + UVA light) involves either oral or topical application of psoralen or a psoralen derivative in combination with UVA irradiation (320−400 nm). In vitro experiments has shown that psoralens penetrate living cells very rapidly within minutes and can be found in all cell compartments.[2] Particularly, 8-MOP was found to be localized in the nucleus and in the cytoplasm of all cells of the different layers of the epidermis of psoriatic skin.[3] It is well-known that photoactivated psoralen molecules modify nucleic acids, proteins and lipids.[4] One of the major mechanisms with respect to DNA photodamage is photobinding, proceeded by an intercalation between DNA base pairs in the dark, followed by monoadduct and potential cross-link formation under UVA irradiation.[4,5] The corresponding cellular effect is the inhibition of nucleic acids synthesis and consequently excessive cell division.[6]

In addition to the interaction with DNA, photoactivated 8-MOP generates singlet oxygen[7] leading to photosensitizing effects of furocoumarins.[6,8] It has been shown in vivo that more than 80% of the bound 8-MOP is localized in proteins and lipids of cells immediately after irradiation with UVA.[9] The ability of 8-MOP to form singlet oxygen is considered to be responsible for a number of side effects in PUVA therapy, such as mutagenicity,[5,10] cell membrane-damaging reactions and, therefore, oedema or erythema,[7,11] and finally inactivation of encymes or of ribosomes.[12] Although the role of singlet oxygen was discussed frequently when using 8-MOP for PUVA therapy, there are hardly any detailed investigations on its generation mainly due to a low quantum yield of 2% or less.

The generation of singlet oxygen by a photoactivated dye usually takes place by the transfer of energy from the triplet state of the dye to molecular oxygen. This energy transfer as well as the relaxation of the involved states is described in detail by the standard model of Parker et al.[13] The model includes the relaxation rates, the rate constants as well as the concentrations of the photoactivated dye, its triplet state, oxygen, singlet oxygen, and of specific quenchers. A noninvasive and precise method to detect singlet oxygen is the measurement of its luminescence at 1.27 μm. Due to the extremely weak signal and the short lifetime of the singlet oxygen luminescence in biological media the investigations are usually performed in solution (e.g., deuterium oxide).

There have been only two reports on the time-resolved measurement of singlet oxygen luminescence generated by photoactivated psoralens.[8,14] However, regarding 8-MOP, the luminescence measurements were performed at the limit of the detector sensitivity and time resolution.[14]

In view of the oxidative role of singlet oxygen in biological media the aim of the present investigation was the detailed evaluation of the energy transfer from the photoactivated 8-MOP to molecular oxygen. Therefore, relevant relaxation rates and several rate constants of the 8-MOP triplet T_1 state as well as

* To whom correspondence should be addressed. Department of Dermatology, University of Regensburg, 93042 Regensburg, Germany. Phone: 49-941-944-9607. Fax: 49-941-944-8943. E-mail: baeumler.wolfgang@klinik.uni-regensburg.de.

[†] Institute of Experimental and Applied Physics.

[‡] Department of Dermatology.

10.1021/jp013727y CCC: $22.00
Published on Web 05/14/2002

the oxygen $^1\Delta_g$ state in deuterium oxide (D_2O) were determined by the analysis of the complete time dependence of the luminescence of singlet oxygen. Moreover, the efficacy of 8-MOP T_1 state deactivation by oxygen, $P_T([O_2])$, which is proportional to the singlet oxygen quantum yield Φ_Δ, was determined at different oxygen concentrations.

2. Experimental Section

2.1. Materials. The compound 8-MOP, Sigma-Aldrich Chemie GmbH (Steinheim, Germany), deuterium oxide (D_2O) with 99.7% atom D, Carl Roth GmbH & Co. (Karlsruhe, Germany), and sodium azide and histidine, Merck KgaA (Darmstadt, Germany), were used without further purification.

2.2. Determination of Oxygen Concentration during Irradiation. Oxygen concentrations were determined measuring the partial vapor pressure of oxygen in solution during irradiation (Licox pO_2, GMS, Kiel, Germany). The temperature of the solution was measured using the corresponding thermocouple. Subsequent application of Henry's law yields the oxygen concentration. Since in the literature there is no Henry's constant of oxygen solved in D_2O, we used Henry's constant for oxygen solved in H_2O for the calculation of the oxygen concentration. To achieve oxygen partial vapor pressures and thus concentrations different from the equilibrium between solution and atmosphere, the solutions were flowed prior to irradiation with oxygen to increase the oxygen concentration or with nitrogen to decrease the oxygen concentration. The oxygen partial vapor pressures ranged from 15 to 273 Torr, corresponding to an oxygen concentration range in solution of 0.026 mM to 0.508 mM.

2.3. Preparation of 8-MOP Solutions. Solutions of 8-MOP in deuterium oxide were prepared by ultrasonic bathing (RK102, Bandelin Electronic KG, Berlin, Germany) 8-MOP crystals in D_2O for 15 min. The concentration of dissolved 8-MOP was thus [8-MOP] = 0.137 mM. Lower concentrations down to 0.0137 mM were achieved by dilution with pure D_2O.

2.4. Luminescence Experiments. The solutions were filled in a flow cell (QS-1000, Hellma Optik, Jena, Germany). 8-MOP was excited using a frequency-doubled dye laser beam (Spectron Laser, Warwickshire, Great Britain, laser dye sulforhodamin 101) pumped by a frequency-doubled Nd:YAG laser with a repetition rate of 10 Hz and a pulse duration of 12 ns (Spectron Laser SL400, Warwickshire, Great Britain). The excitation wavelength was 305 nm with a maximum pulse energy of 2.5 mJ.

2.5. Detection of the Luminescence Signal. The singlet oxygen luminescence signal at 1.27 μm was detected in near-backward direction with respect to the excitation beam using an infrared sensitive photomultiplier (RR5509−42, Hamamatsu Photonics Deutschland GmbH, Germany). For selection of wavelength, two interference filters with maximum transmission at 1.27 μm and half-widths of 25 nm (Schott, Mainz, Germany) and 13 nm (L. O. T. Oriel GmbH & Co. KG, Germany) as well as a dielectric infrared long-pass filter with the edge at 1.11 μm (L. O. T. Oriel GmbH & Co. KG, Germany) were used. Due to the low singlet oxygen luminescence intensity, the luminescence signal was summed up over 10000 laser pulses for each single experiment, using a 7886S Dual Input Multiscaler (time-of-flight, Photon Counter, FAST Com Tec GmbH, Oberhaching, Germany) in a personal computer. The time resolution used for the experiments was 16 ns per channel.

3. Results and Discussion

3.1. Theoretical Considerations. Figure 1 shows the energy transfer model used for this work. Compared to the entire set

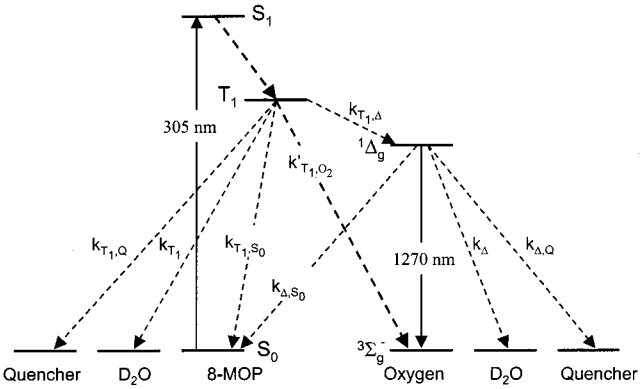

Figure 1. This energy level diagram is valid for the energy transfer processes between the photosensitizer 8-MOP, oxygen, solvent, and quencher.

of energy transfer processes given by Wilkinson et al.,[15] all energy transfer processes from 8-MOP S_1 state to ground-state oxygen were not considered due to the high energy level of the S_1 state of 2.72 eV[16] and a fluorescence lifetime of a few nanoseconds.[17] The energy transfer rate constants between the relevant states are denoted by $k_{i,j}$ [s^{-1} M^{-1}]. k_{T_1} and k_Δ [s^{-1}] denote the reciprocal lifetimes of 8-MOP-triplet and oxygen-singlet state in pure solvent without any further quenching processes. The quenching rate constant k_{T_1,O_2} of the T_1 state by oxygen is given by $k_{T_1,O_2} = k_{T_1,\Delta} + k'_{T_1,O_2}$ where $k_{T_1,\Delta}$ describes the energy transfer to the $^1\Delta_g$ state of oxygen and k'_{T_1,O_2} all other possible quenching processes. According to this energy transfer diagram, the following equations for the concentrations of the 8-MOP triplet T_1 state [T_1] and singlet oxygen [$^1O_2$] can be obtained:

$$\frac{d[T_1]}{dt} = -(k_{T_1} + k_{T_1,S_0}[S_0] + k_{T_1,Q}[Q] + k_{T_1,O_2}[^3O_2])[T_1] = -K_{T_1}[T_1] \quad (1)$$

$$\frac{d[^1O_2]}{dt} = k_{T_1,\Delta}[T_1][^3O_2] - (k_\Delta + k_{\Delta,S_0}[S_0] + k_{\Delta,Q}[Q])[^1O_2] = k_{T_1,\Delta}[T_1][^3O_2] - K_\Delta[^1O_2] \quad (2)$$

Hereby, [$^3O_2$] denotes the concentration of ground-state oxygen and [S_0] denotes the concentration of 8-MOP molecules in the ground state. [Q] is the quencher concentration. The solution of the equations above yields:

$$[T_1](t) = [T_1^0]\exp(-K_{T_1}t) \quad (3)$$

$$[^1O_2](t) = [T_1^0]\frac{k_{T_1,\Delta}[^3O_2]}{K_{T_1} - K_\Delta}(\exp(-K_\Delta t) - \exp(-K_{T_1}t)) \quad (4)$$

with K_{T_1} and K_Δ defined in eqs 1 and 2, respectively. [T_1^0] denotes the initial concentration of the 8-MOP-triplet state immediately after the laser pulse.

Since the singlet oxygen quantum yield is low (Φ_Δ ranges from 0.01 to 0.035 for different aerated solvents[18−20]), the concentration of ground-state oxygen [$^3O_2$] is approximately equal to the oxygen concentration [O_2] measured. Since the fluorescence lifetime τ_F of 8-MOP is a few nanoseconds,[17] the saturation intensity $I_{sat} = h\nu_L/\sigma\tau_F$[21] for the S_0-S_1 transition of 8-MOP is of the order of 10^7 W/cm^2 (h, Planck's constant; ν_L=

c_0/λ_L, laser frequency; c_0, vacuum light velocity; and $\sigma = 4.5 \times 10^{-17}$ cm^2, ground-state absorption cross section). The laser intensity used is in the range of 10^5 W/cm^2. This estimation together with the low triplet quantum yield of $\Phi_{T_1} = 0.06$[22−24] leads to the approximation that the concentration of 8-MOP in the S_0 singlet state is equal to the 8-MOP concentration in solution. Hence

$$K_{T_1} = k_{T_1} + k_{T_1,8MOP}[8MOP] + k_{T_1,Q}[Q] + k_{T_1,O_2}[O_2] \quad (5)$$

and

$$K_\Delta = k_\Delta + k_{\Delta,8MOP}[8MOP] + k_{\Delta,Q}[Q] \quad (6)$$

For low quencher concentrations the total relaxation rate of the T_1 state of 8-MOP is larger than that of singlet oxygen ($K_{T_1} > K_\Delta$). Therefore, according to eq 4, the singlet oxygen concentration $[^1O_2]$ increases exponentially with the relaxation rate K_{T_1} of the T_1 state for times $t \ll 1/K_\Delta$ and decays exponentially with the relaxation rate K_Δ of singlet oxygen for times $t \gg 1/K_{T_1}$. The measured time-resolved luminescence signal was fitted with the function $[^1O_2](t)$ given by eq 4 yielding the values for K_{T_1} and K_Δ. The rate constants for the relaxation of the 8-MOP triplet and oxygen singlet state were obtained by fitting eqs 5 and 6 to the experimentally determined rise and decay rates K_{T_1} and K_Δ, as recently shown with photofrin.[25]

Using the definition of Wilkinson et al.[15] and the assumption of a negligible energy transfer from the 8-MOP S_1 state to oxygen, the singlet oxygen quantum yield Φ_Δ is given by

$$\Phi_\Delta([O_2]) = \Phi_{T_1} f_\Delta{}^T P([O_2]) \quad (7)$$

Here, Φ_{T_1} is the triplet quantum yield. The fraction of the T_1 population quenched by oxygen yielding singlet oxygen is given by

$$f_\Delta{}^T = \frac{k_{T_1,\Delta}}{k_{T_1,O_2}} \quad (8)$$

The proportion of T_1 population quenched by oxygen depends on the oxygen concentration is calculated as follows:

$$P_T([O_2]) = \frac{k_{T_1,O_2}[O_2]}{K_{T_1}([O_2])} \quad (9)$$

where K_{T_1} is given by eq 5. In the experiments k_{T_1,O_2} and K_{T_1} were determined, which is necessary for the calculation of the efficacy P_T of the T_1 state deactivation by oxygen.

3.2. The Detection of Singlet Oxygen. First, the time dependence of the luminescence signal of singlet oxygen in deuterium oxide was investigated. The logarithmic plot of the luminescence signal of singlet oxygen generated by photoactivated 8-MOP ([8-MOP] = 0.137 mM) in D_2O is shown in Figure 2, without any and with the addition of a specific singlet oxygen quencher (sodium azide, concentration $[NaN_3] = 0.1$ mM). The use of the quencher significantly shortened the decay time of the singlet oxygen luminescence from 61 μs to 19 μs, whereas the rise time was constant within the experimental accuracy. Since the luminescence is proportional to the singlet oxygen concentration, eq 4 was used for fitting the experimental results (solid lines in Figure 2). From the fitting functions the rise and decay rates K_{T_1} and K_Δ were determined.

3.3. The Detection of Singlet Oxygen at Different 8-MOP Concentrations. In Figure 3 the Stern−Volmer plot shows the dependence of K_{T_1} and K_Δ on the concentration of 8-MOP. The oxygen concentration in solution during these experiments was $[O_2] = (0.21 \pm 0.02)$ mM. Therefore, according to Henry's law, the solution was in equilibrium with the atmosphere with respect to its oxygen content (aerated). When increasing the 8-MOP concentration from 0.0137 to 0.137 mM the singlet oxygen relaxation rate K_Δ increased linearly. According to eq 6 the slope of the linear fit curve yields the quenching rate constant of singlet oxygen by 8-MOP of $k_{\Delta,8MOP} = (27 \pm 10) \times 10^6$ s^{-1} M^{-1}. Extrapolation to zero 8-MOP concentration yields the lifetime of singlet oxygen in pure deuterium oxide to be $\tau_\Delta = 1/k_\Delta = 67 \pm 3$ μs (see Table 1 for literature values).

The relaxation rate K_{T_1} of the 8-MOP triplet T_1 state (Figure 3), however, remained constant within the experimental accuracy when increasing the concentration of 8-MOP. The value was 0.44 ± 0.04 μs^{-1} for the total T_1 triplet relaxation rate K_{T_1} of 8-MOP in deuterium oxide at the oxygen concentration mentioned above. No values for 8-MOP triplet relaxation rates in D_2O have been found in the literature and the values for 8-MOP triplet relaxation rates in H_2O are ranging from 0.25 to 2.5 μs^{-1} [22,26] without specification of the oxygen concentration. With respect to eq 5 the latter is important for comparison of experimental data. The relaxation rate constant $k_{T_1,8MOP}$ for the quenching of the triplet T_1 state of 8-MOP by 8-MOP is

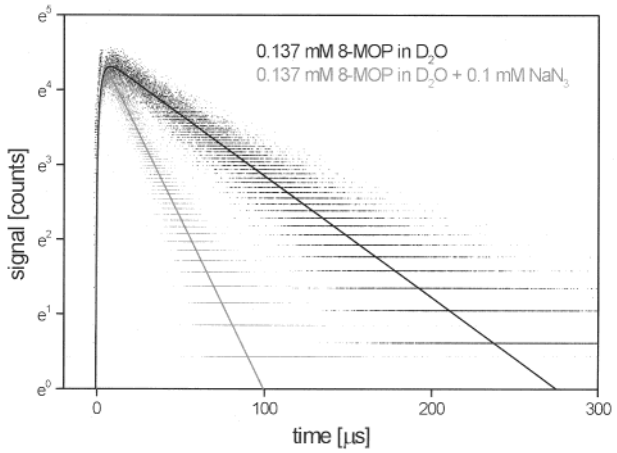

Figure 2. Singlet oxygen luminescence signal vs time for 8-MOP in deuterium oxide with and without addition of the quencher sodium azide. From the measured data points the respective mean background noise has been subtracted. The solid curves have been fitted to the experimental data points using eq 4.

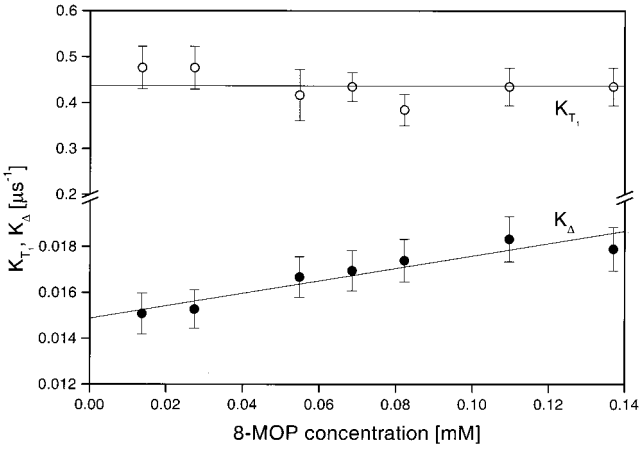

Figure 3. Dependence of the relaxation rates K_{T_1} and K_Δ of the triplet state of 8-MOP and of singlet oxygen, respectively, on the concentration of 8-MOP. The solid curves have been fitted to the experimental data points using eq 5 and 6. Note the axis break in the ordinate scale.

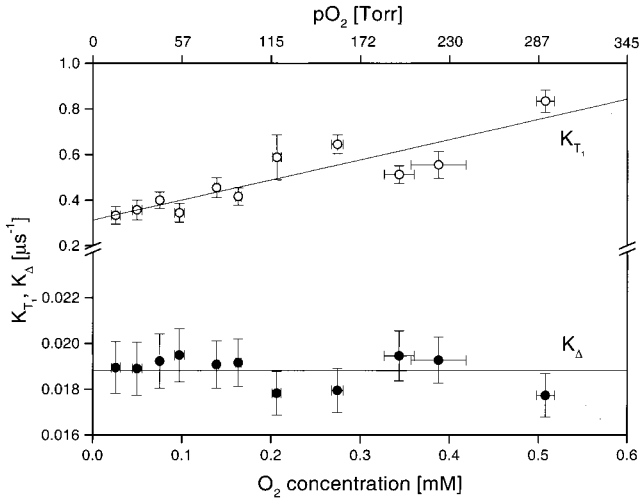

Figure 4. Dependence of the relaxation rates K_{T_1} and K_Δ of the triplet state of 8-MOP and of singlet oxygen, respectively, on the oxygen concentration and partial vapor pressure. The values are shown with respect to the lower (mM) and upper abscissa (Torr). The solid curves have been fitted to the experimental data points using eq 5 and 6. Note the axis break in the ordinate scale.

estimated from the error bars in Figure 3 using eq 5 to be $k_{T_1,8MOP} < 0.6 \times 10^9\ s^{-1}\ M^{-1}$. This value is much smaller than that given in,[22] $k_{T_1,8MOP} = 3.8 \times 10^9\ s^{-1}\ M^{-1}$ and even smaller than the estimated value given in,[24] $k_{T_1,8MOP} = 1 \times 10^9\ s^{-1}\ M^{-1}$.

3.4. The Detection of Singlet Oxygen at Different Oxygen Concentrations. Using a 8-MOP concentration 0.137 mM reveals that the relaxation rate of the 8-MOP triplet T_1 state K_{T_1} shows a linear dependence on the oxygen concentration ($[O_2] = 0.026$ mM to 0.508 mM) (Figure 4). For comparison, the scale of the corresponding oxygen partial vapor pressure (pO_2) in solution for a mean temperature of 24 °C is also shown. According to eq 5 the slope of the linear fit of the data yields the rate constant k_{T_1,O_2} for the quenching of the triplet T_1 state of 8-MOP by oxygen, $k_{T_1,O_2} = (9 \pm 4) \times 10^8\ s^{-1}\ M^{-1}$. This value has been determined for the first time. Extrapolation to zero oxygen concentration, $[O_2] = 0$, yields the relaxation rate of 8-MOP triplet state $K_{T_1} = k_{T_1} + k_{T_1,8MOP}[8MOP] = 0.31 \pm 0.04\ \mu s^{-1}$.

Using the value of K_{T_1}, the concentration of 8-MOP (0.137 mM) and the estimation of $0 \le k_{T_1,8MOP} < 0.6 \times 10^9\ s^{-1}\ M^{-1}$ (see above), the lower limit for the relaxation rate k_{T_1} of the triplet T_1 state of 8-MOP in pure deuterium oxide is estimated to be $0.23 \pm 0.04\ \mu s^{-1}$. This leads to $0.19\ \mu s^{-1} < k_{T_1} \le 0.35\ \mu s^{-1}$ with a mean value of $k_{T_1} = 0.27 \pm 0.08\ \mu s^{-1}$ corresponding to a triplet T_1 lifetime of $\tau_{T_1} = 3.7 \pm 1.1\ \mu s$. These values are also given in Table 1. According to Figure 4, the relaxation rate K_Δ of singlet oxygen is unaffected by variation of oxygen concentration within the experimental accuracy and $K_\Delta = 0.0188 \pm 0.0007\ \mu s^{-1}$ for the 8-MOP concentration given above.

3.5. The Effect of Quenchers on 8-MOP Triplet T_1 State and Singlet Oxygen Relaxation. In Figure 5 the relaxation rates of singlet oxygen and 8-MOP triplet state are shown for different concentrations of sodium azide (10^{-3}−0.1 mM) or histidine (10^{-3}−0.5 mM). The concentration of 8-MOP was 0.137 mM and the concentration of oxygen in solution was (0.21 ± 0.02) mM, indicating equilibrium with the atmosphere according to Henry's law. The triplet T_1 relaxation rate K_{T_1} of 8-MOP is within the experimental accuracy independent of sodium azide ($0.44 \pm 0.04\ \mu s^{-1}$) or histidine concentration ($0.47 \pm 0.04\ ms^{-1}$) and comparable to the value in Figure 3. Using eq 5, from the scattering of the data points and the error bars in Figure

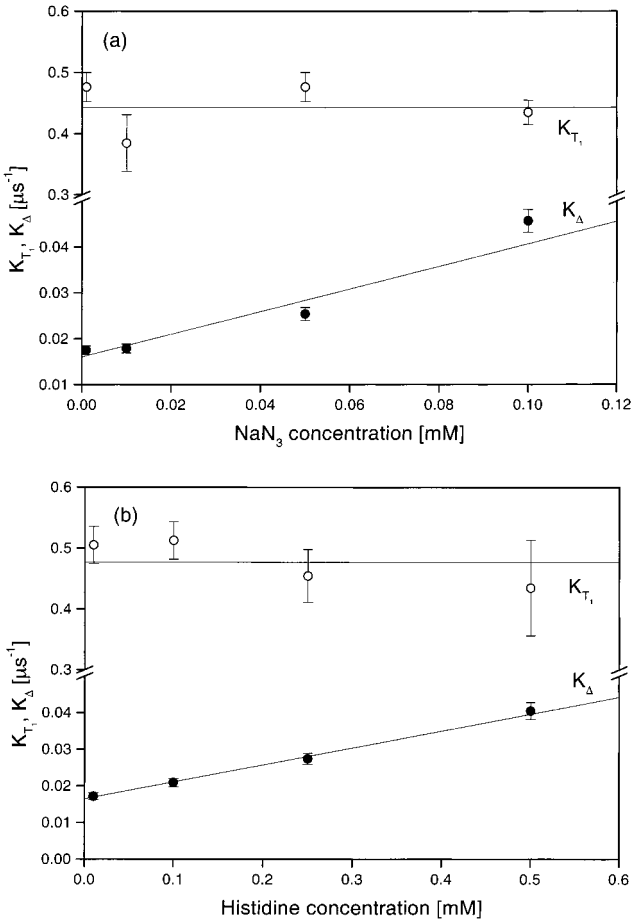

Figure 5. Dependence of the relaxation rates K_{T_1} and K_Δ of the triplet state of 8-MOP and of singlet oxygen, respectively, on the concentration of the quenchers. (a) Sodium azide and (b) histidine. The solid curves have been fitted to the experimental data points using eq 5 and 6. Note the axis break in the ordinate scale.

5 an upper limit for the quenching rate constant $k_{T_1,NaN_3} < 8 \times 10^8\ s^{-1}M^{-1}$ for sodium azide and $k_{T_1,His} < 2 \times 10^8\ s^{-1}M^{-1}$ for histidine is estimated regarding the quenching of the triplet T_1 state of 8-MOP by the respective quencher. Figure 5 shows the linear dependence of the singlet oxygen relaxation rate K_Δ with respect to the quencher concentrations yielding the quenching rate constant $k_{\Delta,NaN_3} = (2.5 \pm 0.6) \times 10^8\ s^{-1}\ M^{-1}$ of sodium azide and $k_{\Delta,His} = (4.6 \pm 0.4) \times 10^7\ s^{-1}\ M^{-1}$ of histidine according to eq 6 (see Table 1 for literature values).

3.6. The Efficacy of the Deactivation of the T_1 State by Oxygen. For several years the role of reactive oxygen species such as superoxide radicals and singlet oxygen have been discussed frequently when using 8-MOP for PUVA therapy.[6−12]

To assess the role of singlet oxygen in photosensitized reactions the efficacy of singlet oxygen generation by the dye used must be determined.[27] In the first step, the efficacy P_T of the T_1 state deactivation by oxygen was determined by applying eqs 5 and 9 to the measured relaxation rate constants. An aerated solution ($[O_2] \approx 0.21$ mM) yields $P_T^{ae} = 0.3 \pm 0.1$. Next, an upper limit F_D^{max} of the singlet oxygen quantum yield is estimated by assuming that the oxygen induced quenching of the T_1 state leads exclusively to the generation of singlet oxygen, i.e., $f_\Delta^T = 1$ [eq 8]. $\Phi_D^{max} = 0.019 \pm 0.007$ for an aerated solution is calculated when using the literature value of the triplet quantum yield $\Phi_{T_1} = 0.06$.[22,23,24] This value is in good agreement with $\Phi_\Delta = 0.02 \pm 0.006$ or ref 18 and similar to the respective value in H_2O (0.01).[23]

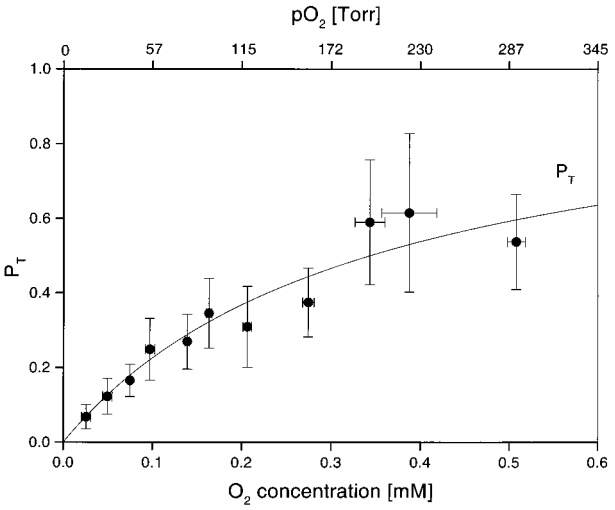

Figure 6. Dependence of the efficacy P_T of 8-MOP T_1 state deactivation by oxygen on its concentration and the corresponding partial vapor pressure. The values are shown with respect to the lower (mM) and upper abscissa (Torr). The solid curve has been fitted to the experimental data points using eq 9.

TABLE 1: Lifetimes τ, Relaxation Rates k and Quenching Rate Constants $k_{i,j}$ of the Triplet T_1 State of 8-MOP and Singlet Oxygen in D_2O[a]

figure in D_2O	this work	literature
k_{T_1} [μs^{-1}]	0.27 ± 0.08	0.25−2.5[15,23]
τ_{T_1} [μs]	3.7 ± 1.1	4.0−0.4[15,22]
k_{T_1,O_2} [$s^{-1}M^{-1}$]	$(9 \pm 4) \times 10^8$	
$k_{T_1,8MOP}$ [$s^{-1}M^{-1}$]	$<0.6 \times 10^9$	3.8×10^9 in methanol[22] 1×10^9 in ethanol[24]
$k_{T_1,NaN3}$ [$s^{-1}M^{-1}$]	$<8 \times 10^8$	
$k_{T_1,His}$ [$s^{-1}M^{-1}$]	$<2 \times 10^8$	
k_Δ [μs^{-1}]	$(1.49 \pm 0.07) \times 10^{-2}$	$(1.5-2.3) \times 10^{-2}$ [15]
τ_Δ [μs]	67 ± 3	67−43 [15]
$k_{\Delta,8MOP}$ [$s^{-1}M^{-1}$]	$(27 \pm 10) \times 10^6$	5.6×10^3 in CCl_4[15]
$k_{\Delta,NaN3}$ [$s^{-1}M^{-1}$]	$(2.5 \pm 0.6) \times 10^8$	$(0.5-8.2) \times 10^8$ [15]
$k_{\Delta,His}$ [$s^{-1}M^{-1}$]	$(4.6 \pm 0.4) \times 10^7$	$(4-93) \times 10^7$ [15]
aerated solution:		
P_T	0.3 ± 0.1	
upper limit ϕ_Δ^{max}	0.019 ± 0.007	0.01 in benzene[8] 0.02 in D_2O[19] 0.035 in PBD[20]

[a] The presented values have been determined from the fits of the *individual* figures using eqs 5 and 6 as described in the text. The error limits have been chosen large enough to get satisfactory agreement between experiments and calculations in *all* figures.

The value of f_Δ^T depends on the triplet state energy E_{T_1} and the polarity of the solvent. For photochemically stable triplet sensitizers f_Δ^T is in the range of 0.25−1.[28] To our knowledge, f_Δ^T has not yet been determined for 8-MOP in D_2O. However, it is important to notice that, according to eq 7, the singlet oxygen quantum yield Φ_Δ is proportional to the efficacy P_T and has the same dependence on the oxygen concentration.

The efficacy of the 8-MOP triplet T_1 state deactivation by oxygen, P_T, for the complete range of the oxygen concentrations are shown in Figure 6. The corresponding oxygen partial vapor pressures (pO_2) in solution for a mean temperature of 24 °C are also shown for comparison. The solid line indicates the fitting function using eq 9 and the values given in Table 1.

The value of P_T might differ when using different solvents (e.g., biological media), but the fact that P_T and therefore any singlet oxygen quantum yield decreases with decreasing oxygen partial pressure is independent of the solvent. Thus, the observed decrease of P_T with decreasing oxygen concentration has an impact on the efficacy of the singlet oxygen generation by a photoactivated dye such as 8-MOP. With respect to 8-MOP and singlet oxygen, a variety of experiments were performed in solution and in vitro under aerated conditions[7−12,14−18] implicating an oxygen partial vapor pressure of about 130 Torr. Recently, Liu et al.[29] stated that singlet oxygen is the principal reactive oxygen species involved in oxidative DNA damage by PUVA treatment. The authors measured a 6-fold increase of 8-hydroxy-2′-deoxyguanosine when calf thymus DNA was incubated with 8-MOP and irradiated, however, under aerated conditions (∼130 Torr).

PUVA therapy is performed under in vivo conditions showing an oxygen partial pressure remarkably lower than in vitro or in solution. Baumgärtl et al.[30] showed that the oxygen partial pressure at the dermal-epidermal junction is only 20 Torr or even less inside the cells. With respect to Figure 6, P_T decreases 4-fold from ∼0.02 at 130 Torr to ∼0.005 at 20 Torr when measured in D_2O. Therefore, Φ_Δ also decreases 4-fold within this oxygen concentration range independent of the actual value of f_Δ^T.

4. Conclusion

The generation of singlet molecular oxygen by photoactivated 8-methoxypsoralen and its relaxation in solutions of D_2O has been investigated in detail by time-resolved near-infrared spectroscopy. The relevant relaxation rates and several rate constants of the involved 8-MOP triplet T_1 state and oxygen $^1\Delta_g$ state were determined and compared with literature values as far as available. Furthermore, the present investigation provides evidence that the quantum yield Φ_Δ and therefore the efficacy of singlet oxygen generation depends critically on the respective oxygen partial pressure. Since this is valid for all solvents, one must be careful regarding the transfer of results and conclusions from experiments in vitro or in solution to experiments in vivo.

References and Notes

(1) Jones, S. G.; Young, A. R.; Truscott, T. G. *J. Photochem. Photobiol. B: Biol.* **1993**, *21*, 223.

(2) Moreno, G.; Salet, C.; Kohen, C.; Kohen, E. *Biochim. Biophys. Acta* **1982**, *721*, 109.

(3) Moreno, G. *Biochimie* **1986**, *68*, 869.

(4) Gasparro, F. P. *Extracorporal Photochemotherapy: Clinical Aspects and the Molecular Basis for Efficacy*; R. G. Landes Company: Austin, 1994; Chapters 2 and 3.

(5) Beijersbergen van Henegouwen, G. M. J.; Wijn, E. T.; Schoonderwoerd, S. A.; de Vries, H.; Dall'Acqua, F. *Z. Naturforsch.* **1989**, *44c*, 819.

(6) Potapenko, A. Ya. *J. Photochem. Photobiol. B: Biol.* **1991**, *9*, 1.

(7) de Mol, N. J.; Beijersbergen van Henegouwen, G. M. J. *Photochem. Photobiol.* **1979**, *30*, 331.

(8) Knox, C. N.; Land, E. J.; Truscott, T. G. *Photochem. Photobiol.* **1986**, *43*, 359.

(9) Sousa, C.; Sá e Melo, T.; Mazière, J.-C.; Santus, R. *Photochem. Photobiol.* **1998**, *67*, 561.

(10) de Mol, N. J.; Beijersbergen van Henegouwen, G. M. J. *Photochem. Photobiol.* **1981**, *33*, 815.

(11) Pathak, M. A.; Joshi, P. C. *Biochim. Biophys. Acta* **1984**, *798*, 115.

(12) Vedaldi, D.; Dall′Acqua, F.; Gennaro, A.; Rodighiero, G. *Z. Naturforsch.* **1983**, *38c*, 866.

(13) Parker, J. G.; Stanbro, W. D. Dependence of Photosensitized Singlet Oxygen Production Porphyrin Structure and Solvent. In *Porphyrin localisation and Treatment of Tumors*; Alan R. Liss, Inc.: New York, 1984; pp 259−284.

(14) Beaumont, P. C.; Rodgers, M. A. J.; Parsons, B. J.; Phillips, G. O. *Photochem. Photobiol.* **1985**, 42.

(15) Wilkinson, F.; Helman, W. P.; Ross, A. B. *J. Phys. Chem. Ref. Data* **1995**, *24*, 663.

(16) Bensasson, R. V.; Land, E. J.; Truscott, T. G. *Excited states and Free Radicals in Biology and Medicine*; Oxford University Press: New Yrok, 1993; p 272.

(17) Andreoni, A.; Cubeddu, R.; Dall′Aqua, F.; Knox, C. N.; Truscott, T. G. *Chem. Phys. Lett.* **1985**, *114*, 329.

(18) Jones, S. G.; Young, A. R.; Truscott, T. G. *J. Photochem. Photobiol. B: Biol.* **1993**, *21*, 223.
(19) Krasnovsky, A. A., Jr.; Sukhorukov, V. L.; Egorov, S. Yu.; Potapenko, A. Ya. *Stud. Biophys.* **1986**, *114*, 149.
(20) Blan, Q. A.; Grossweiner, L. I. *Photochem. Photobiol.* **1987**, *45*, 177.
(21) Hercher, M. *Appl. Opt.* **1967**, *6*, 947.
(22) Craw, M.; Bensasson, R. V.; Ronfard-Haret, J. C.; Sa e Melo, M. T.; Truscott, T. G. *Photochem. Photobiol.* **1983**, *37*, 611.
(23) Grossweiner, L. I. *The Science of Phototherapy*; CRC Press: Boca Raton, 1994.
(24) Sá e Melo, M. T.; Averbeck, D.; Bensasson, R. V.; Land, E. J.; Salet, C. *Photochem. Photobiol.* **1979**, *30*, 645.
(25) Kilger, R.; Maier, M.; Szeimies, R. M.; Bäumler, W. *Chem. Phys. Lett.* **2001**, *343*, 543.
(26) Poppe, W.; Grossweiner, L. I. *Photochem. Photobiol.* **1975**, *22*, 217.
(27) Tanielian, C.; Schweitzer, C.; Mechin, R.; Wolff, C. *Free Radical Biol. Med.* **2001**, *30*, 208.
(28) Schmidt, R.; Shafii, F. *J. Phys. Chem. A* **2001**, *105*, 8871.
(29) Liu, Z.; Lu, Y.; Lebwohl, M.; Wie, H. *Free Radical Biol. Med.* **1999**, *27*, 127.
(30) Baumgärtl, H.; Ehrly, A. M.; Saeger-Lorenz, K.; Lübbers, D. W. *Initial results of Intracutaneous Measurements of PO_2 Profiles*. In *Clinical Oxygen Pressure Measurement*; Ehrly, A. M., Hauss, J., Huch, R., Eds.; Springer-Verlag: Berlin, 1987.